Micron 103 (2017) 90–98

Contents lists available at ScienceDirect

Micron

journal homepage: www.elsevier.com/locate/micron

Research article

Characterization and morphological analysis of individual aerosol of PM_{10} in urban area of Lucknow, India

Sushil Kumar Bharti[a], Dhananjay Kumar[a], Sangeeta Anand[a], Poonam[a], Shymal Chandra Barman[b], Narendra Kumar[a,*]

[a] Department of Environmental Science, Babasaheb Bhimrao Ambedkar University, Lucknow, 226025, Uttar Pradesh, India
[b] Environmental Monitoring Division, Indian Institute of Toxicology Research, Mahatma Gandhi Marg, Lucknow, 226 001, Uttar Pradesh, India

ARTICLE INFO

Keywords:
Aluminosilicates
NAAQS
Particulate matter
SEM-EDS
Soot
Tar balls

ABSTRACT

Airborne particulate matters were collected during the period of October 2015 to September 2016 in Lucknow at different sampling sites. The annual mean concentration of particulate matter was found to be relatively higher than the limits prescribed by National ambient air quality standards (NAAQS), United State Environmental Protection Agency (USEPA) and World Health Organization (WHO). Particulate matters were studied for morphological analysis, elemental composition and functional group variability with the help of Scanning Electron Microscope-Energy Dispersive Spectroscopy (SEM-EDS) followed by Fourier Transform Infrared spectroscopy (FTIR). Morphological characteristics viz. particle count, aspect ratio, circulatory, roundness, equivalent spherical diameter (ESD) and surface area revealed that the particles were perfectly spherical to irregular in shape. Based on the morphology and elemental composition, four clusters of a particulates namely organic particle with inorganic inclusion, soot, tar balls and aluminosilicates were found. FTIR spectra revealed the presence of sulfate, bisulfate, particulate water, silicate, ammonium, aliphatic carbon, aliphatic alcohol, carbonyl and organic nitrates.

1. Introduction

Over past few decades, emission of particulate matter (PM) in urban environment is recognized as a major threat to human health. Contribution of anthropogenic sources to the aerosol load in urban atmosphere has increased significantly in recent past, which in turn enhanced the incidences of cardiopulmonary disorders, skin diseases, lung cancer, and mortality especially in urban areas (Strak et al., 2012; Kumar et al., 2013; Deshmukh et al., 2012a). According to International Agency for Research on Cancer (IARC) various components of particulate matter have been classified as carcinogenic to human health (WHO, 2014). Atmospheric aerosols can absorb organics (soot, elemental carbon and polycyclic aromatic hydrocarbon), inorganic compounds (heavy metals, sulphate and nitrates), acid salts, water, endotoxins, and allergens, which promote mutation and finally lead to cancer (Sielicki et al., 2011). The PM_{10} (airborne particle with aerodynamic diameter less than 10 µm) are generated from soil dust, vehicular exhaust, biomass burning, domestic heating, power plants, smoke stacks and unpaved road dust suspension, however, $PM_{2.5}$ (airborne particle with aerodynamic diameter less than 2.5 µm) are generated from incomplete combustion of petroleum products, road dust, crustal materials, biomass burning and domestic heating (Bond et al., 2011). Threat to human health from aerosol can be categorized according to their penetrating ability into lungs, epithelial cells; however, $PM_{10\text{-}2.5}$ (aerodynamic diameter between 2.5–10 µm) can readily perforate and deposit in extra thoracic region of airways (Berube et al., 2007), whereas $PM_{2.5\text{-}1}$ (aerodynamic diameter between 1- 2.5 µm) can penetrate deep into distal lung which ultimately exacerbate chronic respiratory and cardiovascular diseases (Stevanovic et al., 2013). Particle numbers and surface area plays a pivotal role in determining health hazards due to ultrafine fraction of coarse particulates (Levin et al., 2016). Several studies have been done to determine the concentration of particulate load in atmosphere; however, there is limited information available in literature on chemical composition, size, mixing and morphology of particulate matter, which can provide better understanding about its origin and health effects (Deshmukh et al., 2013; Kumar et al., 2013; Khan et al., 2010; Tecer et al., 2009). Elemental composition of particulate matter plays an important role in characterization of particulate matter (PM) and also provides reliable data for identification of emission sources (Wu et al., 2013). Wide range of techniques (AAS, XRF, INAA, PIXE and ICP-MS) has been used to determine the elemental composition of PM but most of these

* Corresponding author.
E-mail address: narendrakumar_lko@yahoo.co.in (N. Kumar).

http://dx.doi.org/10.1016/j.micron.2017.09.004
Received 5 February 2017; Received in revised form 1 September 2017; Accepted 3 September 2017
Available online 14 September 2017
0968-4328/

techniques do not provide composition according to their specific shapes and sizes (Ram et al., 2012). Therefore, SEM-EDS has been used to identify the source on the basis of their morphological characteristics like perimeter, circulatory, shape, size, equivalent spherical diameter (ESD) and aspect ratio of individual particles (Mishra et al., 2015; Satsangi and Yadav 2014; Kulkarni et al., 2011).

However, separation and quantification of the complex mixture of organics present in atmosphere is the limitation with SEM-EDS. Quantitative measurements of functional groups by FTIR give detailed information on the physical and chemical properties of most of the organic fractions (Gilardoni et al., 2009; Maria et al., 2002). Studies have reported the presence of inorganic groups such as SO_4^{2-}, NO^{3-}, SiO_4^{4-}, and NH^{4+} and organic functional group like aliphatic carbons, carbonyls, and organic nitrates in urban atmosphere (Verma et al., 2014; Khare et al., 2011; Brown et al., 2007; Maria et al., 2002; Blando et al., 1998a, 1998b; Allen et al., 1994). Several studies have been carried out to see the particle morphology, elemental composition and their adverse effects on health (Moffet et al., 2016; Dzepina et al., 2015; Lee et al., 2015; China et al., 2014; Adachi and Buseck, 2011a,b; Cong et al., 2010). However, in Indian context limited studies have reported the presence of carbonaceous particle such as soot, tarballs, alumino-silicates, sulphate and mineral dust in ambient air (Murari et al., 2016; Tiwari et al., 2015; Mishra et al., 2015; Satsangi and Yadav 2014; Ram et al., 2012; Pipal et al., 2011). Lucknow is the capital of densely populated state of India i.e. Uttar Pradesh, where vehicular exhaust is considered as major source of airborne pollution (Sharma et al., 2006; Kisku et al., 2003). In previous years vehicle density has increased from 1709662 to 1864556, which has added enormous load of particulate matter in ambient air (RTO Lucknow, 2016). However, data on characterization of PM in terms of morphological feature, elemental composition, mineral types and potential source is still scanty. Therefore, the present study has been conducted to determine not only the concentration of particulate matter but also their chemical composition and probable pathogenicity.

2. Material and method

2.1. Study area

Lucknow (Urban area/Metropolitan region) is fastest growing city with population of 2,902,920 (Census of India, 2011) and lies between 26° 52′ Latitude and 80° 56′ Longitude at 128 m above sea level (Fig. 1). Being a part of middle Indo Gangetic Plane, the city characteristically experiences humid sub-tropical climate with three distinct season viz. summer (March to June, 38–46 °C), monsoon (July to October) winters (November to February, 3–15 °C). The relative humidity remains very high in monsoon season (70–90%) followed by winter (50–80%) and summer (40–60%) (Fig. 2b). Wind speed and wind direction plays significant role in the dispersion of pollutants and flows from west to northeast (Oct–April) followed by westerly to northwesterly in other months (Fig. 2c). Samples were collected from 6 sampling location across the city (Table 1).

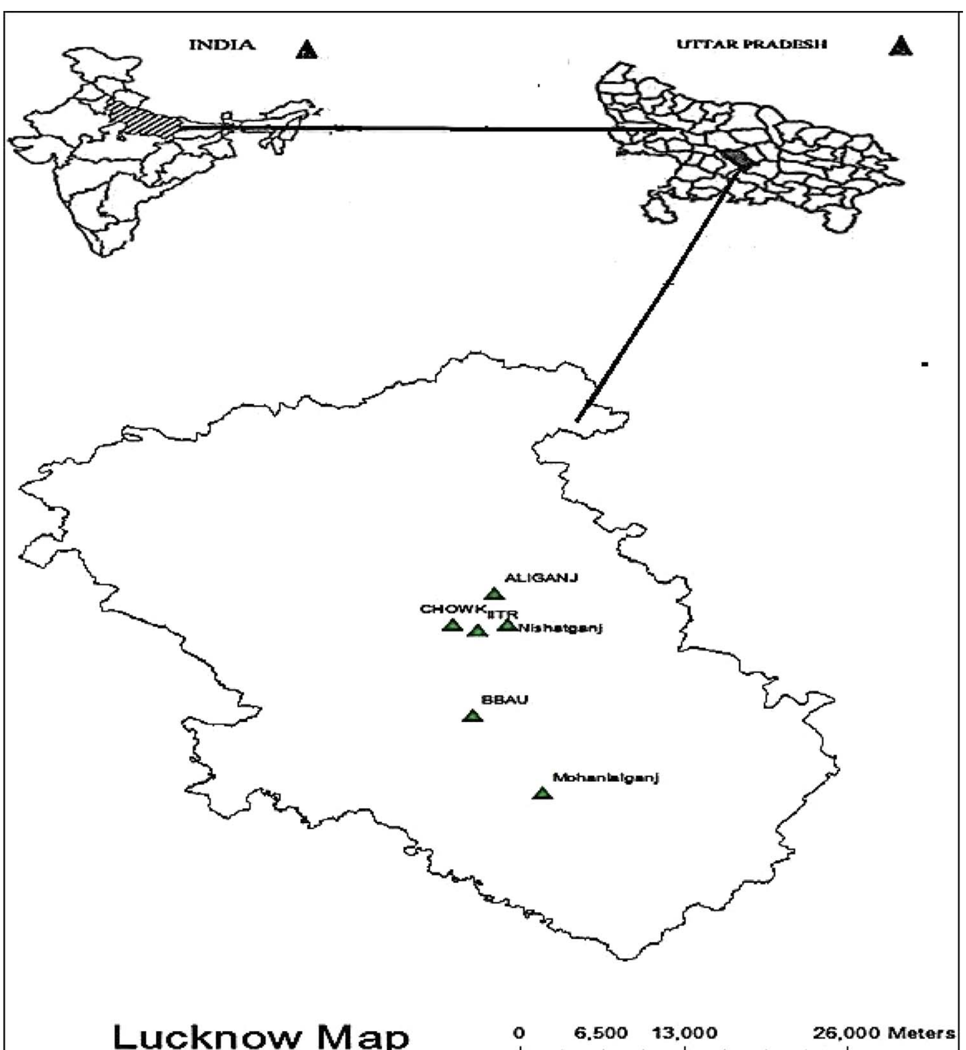

Fig. 1. Different sampling sites at Lucknow.

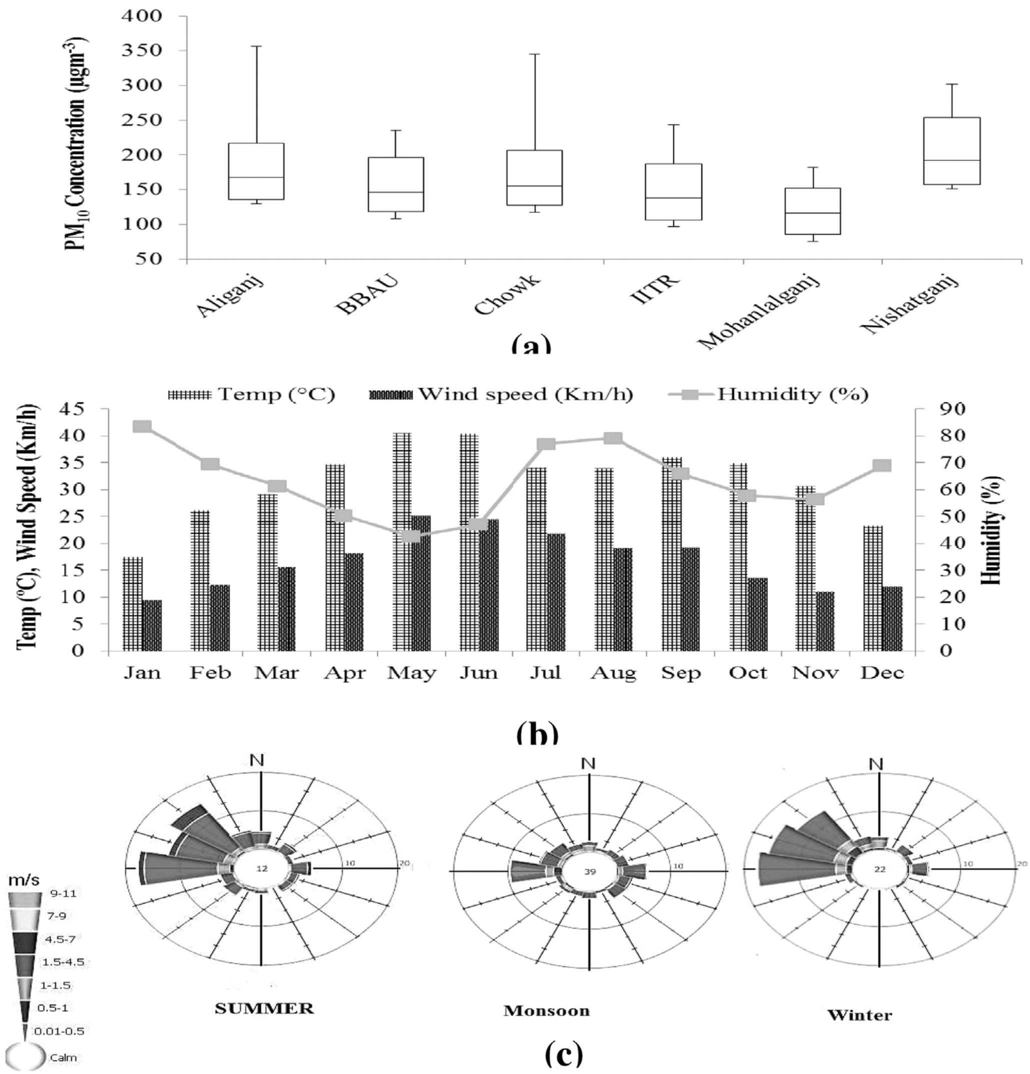

Fig. 2. Temporal variation of PM$_{10}$ and meteorological variables at Lucknow: (a). The annual mean concentration of PM$_{10}$ at the different sampling sites (b) Prevailing meteorological condition; temperature, wind speed, and humidity (c) The wind rose diagram (Source: Indian Meteorological department Lucknow) of Lucknow during study period.

2.2. Sample collection and analysis

Continuous monitoring of PM$_{10}$ was carried out using respirable dust sampler (Mode-460 BL, Envirotech, New Delhi) at a flow rate of 1.1-1.3 m^3/min for 24 h. A total number of 144 samples were collected with respirable dust sampler (Model-460 BL, Envirotech, New Delhi) at a flow rate of 1.1–1.3 m^3/min for 24 h. The collection time was 24 h with one sample per month at every sampling site. The sampling instruments were fixed at breathing height of 6 feet above the ground level. Glass fiber filter of 8 × 10 inches were used for sampling of PM$_{10}$. The filters were equilibrated in desiccators containing silica gel for 24 h before and after sample collection and weighed on pre-calibrated electronic balance (Mettler Toledo, Japan) to determine the weight of dust. A field blank was also generated for each sample collected during the study to monitor the sample contamination during transport and analysis. Field blanks were filters that were transported to and from the field in filter cases with the samples and underwent same gravimetric and FTIR analysis. Afterwards, samples were put in polyethene bags immediately and preserved in refrigerator at 4 °C. The particulate mass concentration was calculated using following formula.

$$PM_{10}(\mu g/m^3)=\frac{fwp - iwp}{v} \times 10^6$$

Where fwp = final weight of filter paper (g)iwp = Initial weight of filter paper (g)v = Total air volume (m^3)10^6 = conversion of g into µg.

2.3. SEM-EDS instrumentation

The morphological and elemental characterization of airborne particles were carried out with the help of computer controlled SEM (JSM

Table 1
Morphological characteristics of particulate matter collected from institutional, rural, and commercial areas of Lucknow.

Sampling Sites	Count	Circulatory	Aspect Ratio	Roundness	ESD	Surface area (µm ^{2})
Site-1(Aliganj)	990	0.8	1.95	0.63	4.56	162.11
Site-2 (BBAU)	547	0.85	1.8	0.69	3.24	104.51
Site-3 (Chowk)	1724	0.79	1.96	0.61	4.63	140.95
Site-4 (IITR)	125	0.84	1.84	0.69	3.23	74.72
Site-5 (Mohanlalganj)	256	0.88	1.85	0.69	2.44	38.03
Site-6 (Nishatganj)	1364	0.82	1.93	0.63	3.47	87.84

6490LV, JEOL, Japan) coupled with EDS (Oxford INCA x-act, UK) having resolution of 3.0 nm. Dry and particle loaded filters were cut in to approximately 1 mm^2 size and mounted on aluminum stubs with double sided sticky carbon tape. A very thin film of Au-Pd was deposited on the surface of the samples using Ion Sputter Coater (JFC 1600, Auto Fine Coater, JEOL, Japan) under argon gas atmosphere. The fine coating of Au-Pd makes the samples electrically conductive. A total of 36 SEM micrograph (6 micrographs from each site) were taken at different magnification viz. 20,000X, 30,000X and 40,000X, while, surface morphology (size and shape) of airborne particles were analyzed by secondary electron detector at 20 kV accelerating voltage. Representative images of each site have been referred to describe the morphological characteristics of airborne particles. The elemental composition of airborne particles was analyzed by EDS (Oxford INCA x-act, UK). EDS spectra of the individual particle was obtained by scanning an electron beam with an accelerating voltage of 15–30 kV to determine the individual elemental composition (Sielicki et al., 2011; Pipal et al., 2011; Srivastava et al., 2009).

2.4. FTIR instrumentation

Particulate matter collected on the filter paper was scrapped with the help of brush and was mixed with potassium bromide. The KBr based pellets were compressed into a thin disk using hydraulic pressure of ten ton (CAP-15T). The absorbance spectrum was measured between 4000 and 400 cm^{-1} at a resolution of 0.09 cm^{-1} using (FTIR Nicolet TM 6700, Make, Thermo Scientific, USA). Final sample spectra were obtained by subtracting the spectra of field blank from the spectra of corresponding sample.

3. Result and discussion

3.1. Variation of PM_{10} and $PM_{2.5}$

The annual mean concentrations of the $PM_{10}$and meteorological variable have been plotted in Fig. 2. The annual mass concentration of coarser particulate matter was found to be 177.63 ± 70.65, 156.89 ± 89.84, 166.49 ± 101.78, 145.27 ± 95.45, 124.0 ± 39.47 and 193.28 ± 121.75 μg m^{-3} at site-1, 2, 3, 4, 5, and 6 respectively (Fig. 2a). The annual mean concentration of PM_{10} was found to be almost three times higher than annual standards (PM_{10}; 60 μ gm^{-3}), prescribed by National Ambient Air Quality Standards (NAAQS, 2009), 1.2 times to the 24 h standards (PM_{10}; 150 μ gm^{-3}) prescribed by United State Environmental Protection Agency (USEPA, 2017) and approximately 7-8 times to the standards (PM_{10}; 20 μg m^{-3}) prescribed by World Health Organization (WHO, 2005). Similar results were also reported from urban atmosphere of other Indian cities viz. Varanasi (53.3–354.7 μg m^{-3}; Sen et al., 2017; Murari et al., 2016), Agra (126.7–231.4 μg m^{-3}; Pachauri et al., 2013), Delhi (63.3–354.7 μg m^{-3}; Sharma et al., 2016), Kanpur (76.9–213 μg m^{-3}; Gargava & Rajagopalan, 2016) and Kolkata (171.5 ± 38.5 μg m^{-3} Sharma et al., 2016), while similar findings were also reported from Paddington (264.7–1066.0 μg m^{-3}; Song et al., 2016), Baotou (17.5–681 μg m^{-3}; Zhou et al., 2016), Rio de Janerio (71–312 μg m^{-3}; Toledo et al., 2008), and Dhaka (10.1–491 μg m^{-3}; Begum et al., 2013). As expected, higher concentration of particulate matter was found in Indo-Gangetic Plains due to its unique geomorphology, and regional micrometeorological conditions, which, do not favor the quick disposal of pollutants, rather traps them in the lower atmosphere (Singh et al., 2017; Tiwari et al., 2012). There are various natural and anthropogenic sources which can elevate the concentration of particulate matter in the atmosphere, but severity of PM have been primarily attributed to combustion of fossil fuels, industrial activities, waste incineration, biomass and crop residue burning, particularly in developing countries (Tiwari et al., 2015).

3.2. SEM image analysis

Approximately 5000 individual particle with Image J software developed by National institute of health, Maryland (Collins, 2007), which yielded important information about morphological features, such as count, total area, average size, perimeter, circularity, aspect ratio, roundness; equivalent spherical diameter (ESD), surface area and volume of PM_{10} (Table 1). This image descriptor was automatically obtained using the software. Primary feature such as aspect ratio (Eq. (1)), defined as the ratio of longest dimension (L_{max}) to the maximum orthogonal width (W_{max}). Aspect ratio used to classify the particle shape i.e. equant, acicular or fibrous. Average AR was found to be in the range of 1.84–1.96 which is recorded for Cl and S bearing particle (Scheuvens et al., 2011). Circulatory (Eq. (2)) is sensitive to boundary irregularity of particle; average circulatory was less than one which indicates that most of the particles are not perfectly spherical (China et al., 2014). Roundness (Eq. (3)) of particle was ranged from 0.61 to 0.70 (mean 0.68), indicates that the particles vary in shape from nearly spherical to irregular. For non-spherical particle a range of equivalent diameter are used and can be expressed as equivalent spherical diameter (Eq. (4)). According to Expert panel on air quality standards (2001), a value of ESD greater than 0.93 is known as respiratory fraction. Large surface area (Eq. (5)) of ultrafine particle increases their interaction with lung tissue and can cause greater damage to lungs. An increase in number of particles simultaneously increases the surface and provides more space for microscopic airborne toxic elements to adhere rapidly (Wu et al., 2008). All dimensional parameters were measured in calibrated units (microns).

$$\text{Aspect Ratio} = L_{max}/W_{max} \quad (1)$$

$$\text{Circulatory} = 4\pi \times A/p^2 \quad (2)$$

$$\text{Roundness} = p^2/4\pi \quad (3)$$

$$\text{EquivalentSphericalDiameter} = 2\sqrt{A}/\pi \quad (4)$$

$$\text{SurfaceArea} = 4\pi \times (ESD/2)^2 \quad (5)$$

3.3. Particle morphology and classification

A total of 5000 particles were analyzed using SEM-EDS and secondary electron imaging. Individual particles were classified into 4 categories viz. organic particles with inorganic inclusion, soot, tar balls, and aluminosilicates on the basis of their chemical composition, surface morphology and relative abundance (Table 2). Based on the relative abundance of weight percentage of the elements, it was found that the entire airborne particles collected from different sites were carbonaceous, i.e. their major element was found present was C (Pósfai et al., 2003). The relative abundance of other elements showed greater variability than C. Since organic particles with inorganic inclusion, soot and aluminosilicates were found present at almost every site, whereas, tar balls were only observed only at site-1, 2 and 6 (Table 2).

3.4. Morphological identification of particle

3.4.1. Group I. Organic particles with inorganic inclusion

Due to lack of typical morphology and micro structural feature of the particles, the most abundant particle was termed as “Organic particles with inorganic inclusion” and was found present at every site (Table 2). However, on the basis of morphology, predominance of organic particles with inorganic inclusion was observed at site-3, 4 and 5 (Fig. 3a, 3b). The organic particles are mainly composed of C and small amounts of O and are stable in the electron beam, whereas, inorganic particles contained crystalline K-salts in the form of KCl or K_2SO_4 (Li et al., 2003). Source of these type of particles varies with fossil fuel combustion, biomass burning and prevailing meteorological condition

Table 2
Relative abundance of organic particles with inorganic inclusions, soot, tar balls and aluminosilicates at different sampling sites of Lucknow.

	Weight% of elements			Relative abundance of particle and their morphology			
Sampling Sites	C- rich	O-rich	Si-Na-Al-rich	Organic Particles with Inorganic Inclusions	Soot	Tar balls	Aluminosilicates
Site-1	47.41	29.88	17.79	+ + +	+ + +	+ + + +	+
Site-2	40.25	37.8	13.44	+ + +	+ + +	+ + + +	+
Site-3	37.6	44.22	13.48	+ + + +	+ + + +	ND	+
Site-4	37.19	40.72	13.00	+ + + +	+ + + +	ND	+
Site-5	32.62	44.03	16.65	+ + + +	+ + + +	ND	+
Site-6	39.16	37.67	13.95	+ + +	+ + +	+ + + +	+

and they are mostly emitted from biomass smoke and regional haze (Berube et al., 1999; Cong et al., 2009; Pósfai and Buseck, 2010; Tumolva et al., 2010). However, their irregular morphology suggested that they were hydrated and organic particles within particle may be highly soluble in water.

3.4.2. Group II. Tar balls

Tar balls having spherical and amorphous structure were found to be present at every site, however, predominance was noticed at site-1, 2 and 6 (Fig. 3a, 3b). Tar balls are stable under electron beam and not typically aggregate with other particles (Pósfai et al., 2003). The fraction of C in tar balls was high with minor amount of atomic oxygen where, O was existing as carboxylic carbonyls, oxygen-substituted alkyl (O-alkyl-C) functional groups, followed by ketonic carbonyls and some contained S, K, Cl and Si (Posfai et al., 2003; Tivanski et al., 2007). Tar balls are most abundant in slightly aged smoke of biomass burning (Pipal et al., 2011; Cong et al., 2009; Zhang et al., 2010).

3.4.3. Group III. Soot Particles

Soot particles exhibit chain like non-fractal agglomerate of the carbonaceous particle (Campos-Ramos et al., 2009; Buseck et al., 2012). Soot have a distinct morphological structure of individual spherules and arranged in wavy graphitic layers (Fig. 2a; 3). The concentration of soot particles were found to be strongly correlated with high traffic density at site-3, 4 and 5 reason being a commercial area in addition to bus and auto (Posfai et al., 1999; Posfai and Molnar, 2000). Based on their morphology and coating three types of soot particles were identified viz. embedded, partly coated and soot with inclusion. The embedded soot (highly coated) are those where, the particle is completely engulfed by organic and inorganic material. They were found present at every site, but they were abundant at site-2, 4 and 6 (Adachi and Buseck 2008; Hand et al., 2010). Partly coated soot was found at site-4 and 6 which, reflects that these particles were not fully engulfed but, their voids are completely filled by coating materials (China et al., 2014, 2013). At site 1, 3 and 5 soot inclusion was observed, where soot particles were intermingled with other particles but not coated by other material (Adachi and Buseck, 2008). Aluminosilicates, quartz, and feldspar mainly composed of Si and Al with a variable amount of Na, K, Mg, Ca, Fe and Ti were also identified at every site (Cuadros et al., 2015; Díaz-Hernández and Párraga, 2008; Engelbrecht et al., 2009a; Jeong et al., 2014).

4. Identification of functional groups by Fourier Transform Infrared Spectroscopy (FTIR)

FTIR absorption spectra revealed the presence of following functional groups; inorganic SO_4^{-2}, HSO^{-4}, H_2O, SiO_4^{-4}, SiO_2, $NO^{-3,}$ SiO_4, and NH_4^+ and organic viz. C—H, R-OH, R-O—N-O and C═O (Table 4 and Fig. 4).

4.1. Composition of inorganic mass

Sulphate is formed in the atmosphere from photo-oxidation of sulphur dioxide (Seinfeld and Pandis, 1998). Sulphate and bisulphate was

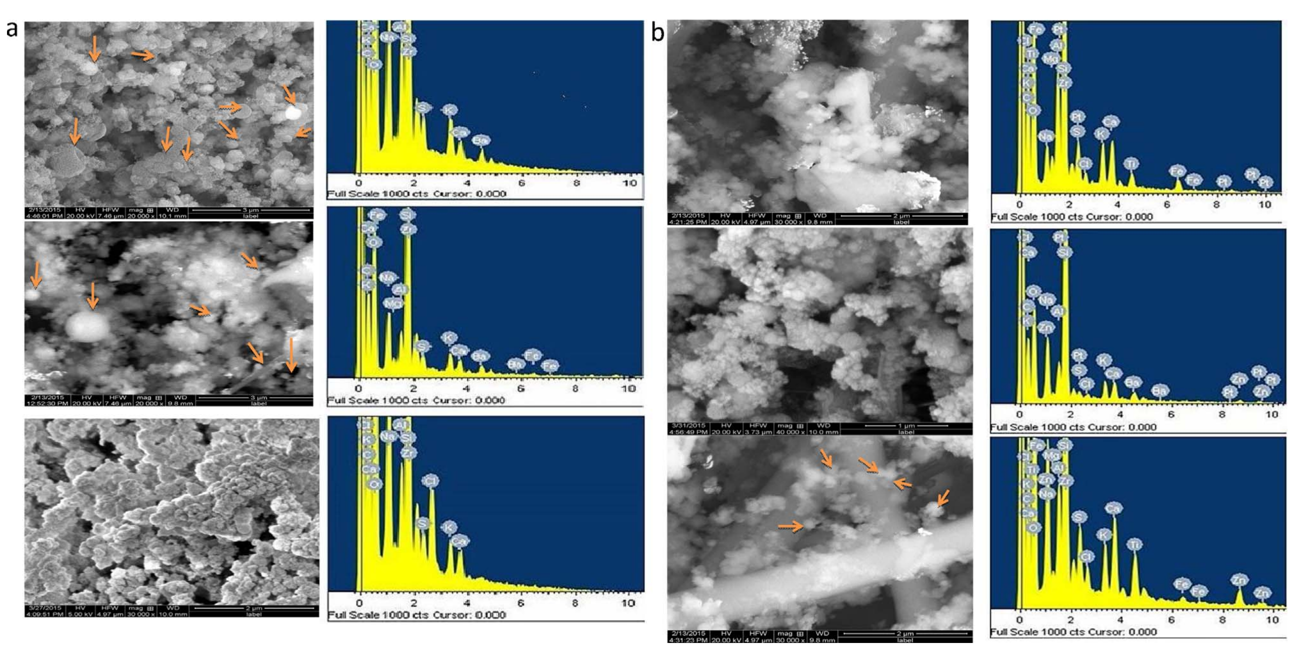

Fig. 3. SEM and EDS spectra of PM_{10} (Site 1, 2 and 3) with greater abundance of organic particles with inorganic inclusions and soot (Site 3), tar balls soot (site 1) and aluminosilicates (Site 1, 2 and 3). (b) SEM and EDS spectra of PM_{10} with organic particles with inorganic inclusions (site 4, 5, and 6), tar balls (site 6), soot (site 4, 5, and 6) and aluminosilicates (site 4, 5 and 6).

Table 3
Comparative statements of the morphological feature of airborne particle and their respective origin.

Area	Particle group identified	Morphology	Source	Origin	References
Mt. Qomolangma (Himalayas)	Soot/tar ball (C abundant, S minor)	Chain aggregation of carbonaceous spherules	Fuels, biomass burning, incomplete fossil fuel combustion	Natural and Anthropogenic	Cong et al. (2010)
	Aluminosilicates	Irregular shape	Soil	Natural	
	Calcium sulfate	Irregular shape	Local crustal source	Natural and anthropogenic	
	Ca/Mg CO3	Irregular shape	Soil	Natural	
	Fe/Ti-rich particles 3%	Irregular shape	Soil	Natural	
	Pb-rich particles	Spherules	Automobile, mining, waste incineration	Anthropogenic	
	Biological particles	Variable morphology	Pollen, bacteria, excrements of insects	Natural	
Portugal (background)	Aluminum silicates	Variable morphology	Soil	Natural	Slezakova et al. (2008)
	Fe oxides and alloys	Variable morphology	Automobile and traffic	Traffic	
	Sulfates (Na & K)–	Variable morphology	Sea	Natural	
	Ti/Al rich Natural	Variable morphology	Soil	Natural	
	Lead sulfate–	Variable morphology	Traffic	Anthropogenic	
Chandigarh, India	Spherical fly ash	Spherical		Traffic	Sharma and Srinivas (2008)
	Silica/Aluminosilicates –	Spherical and nonspherical	Crust	Natural and anthropogenic	
	Clay, quartz, calcite, and gypsum	– Irregular	Soil	Natural and anthropogenic	
	Cubical shaped salt particle –	Cubic	Arabian sea	Natural	
	Biological particles	Spherical and nonspherical	Grass pollens, corn smut	Natural	
Agra, India	Aluminosilicates	Spherical and nonspherical	Crustal	Natural	Pipal et al. (2011)
	Ca rich (CaCO3)		Construction agriculture, natural soil	Natural and anthropogenic	
	C-rich particles (soot and tar balls)	Flaky, chain and small aggregate of spherulite	Gasoline and coal burning	Anthropogenic	
Pune, India	Aluminosilicates	Spherical irregular	Combustion process crustal (soil)	Anthropogenic natural	Satsangi and Yadav (2014)
	Carbonates (CaCO3) Erosion of rocks	Irregular	Erosion of rocks	Natural	
	Halite (NaCl)	Cubic	Sea	Natural	
	Sulfate	Irregular	Biomass burning and fossil fuel	Anthropogenic	
	Soot of fine particles	Agglomerates	Short chain burning and combustion of fossil fuel	Anthropogenic	
Lucknow	Organic particles with inorganic inclusion	No distinct morphology	Biomass smoke and regional haze, fossil fuel combustion	Anthropogenic	In present study
	C-rich particles (soot)	agglomerate of carbonaceous particle	Fuels, biomass burning, incomplete fossil fuel combustion, short chain Burning and combustion of fossil fuel	Anthropogenic	
	Tar balls	spherical, amorphous, and stable in electron beam	Fossil fuel and biomass burning	Anthropogenic	
	Silica/Aluminosilicates	Irregular	Combustion process crustal (soil)	Natural	

found integrated between 1000–1200 cm^{-1} and 605–595.8 cm^{-1} respectively (Table 4 and Fig. 4). Particle water firmly bound to aerosol salts which absorb wavelength at 1600–1700 cm^{-1}, but if water comes from salt hydrates it absorbs the radiation in the range of 3350–3450 cm^{-1}. In present study all the samples have salt hydrates (Tiwary et al., 2008; Blando et al., 1998a, 1998b; Allen et al., 1994). The absorbance peak at 1420–1440 cm^{-1} indicates the presence ammonium ion (Maria et al., 2002). Strong absorption at 1090–730 cm^{-1} represents the dominance of quartz and kaolinite in the particulates (Blanco and McIntyre 1972). Absorption between 461 and 467 cm^{-1}

Table 4
Observed frequencies in the PM_{10} collected from different sites of Lucknow along with their corresponding functional groups.

Functional Group		Absorption frequency (cm^{-1})	References
		INORGANICS	
SiO_4^{2-}	Sulphate ions	1021.5,1023.8,1022.4,1030.6,1072.9,1072.9, 645, 646.2, 1046.9, 1024.8	Brown et al. (2007), Allen et al. (1994)
HSO_4^-	Bisulphate ions	605.2, 595.8	Brown et al. (2007), Allen et al. (1994)
H_2O	Particulate Water	3391, 3409.9, 3401.6, 3405.9, 3405.7	Tiwary et al. (2008), Blando et al. (1998)
NH_4^+	Ammonium ions	1424.9, 1440, 1429.8, 1542.8	Maria et al. (2002)
SiO_4^{4-}	Silicate ions	793.8,777.2,776.8,693.7, 690.7, 783.8, 796.2, 773.8	Blanco and McIntyre (1972)
SiO_2	Silica	466.7, 467.9, 463.4, 467.5, 463.6,465.5	Manoharan et al. (2012), Nayak and Singh (2007), Ko and Chu (2005)
ORGANICS			
C—H	Aliphatic carbons	2920.3, 2850.5, 2924.2, 2922.5, 2853.3, 2923.6, 2922.3, 2922.6 1384.2, 1385.3, 1384.4, 1384.5	Maria et al. (2002), Shaka and Saliba (2004)
			Santosh and Duarte (1998), Bellamy (1975)
OH	Alcohol	3600, 3622	Saxena et al. (1996)
C=O	Carbonyl carbons	1647.2, 1725.2	Saxena et al. (1996)
C—O-N—O	Organonitrate	1620.8,1647.2,1639,1624, 1629,1616	Anil et al. (2014), Shaka and Saliba (2004)

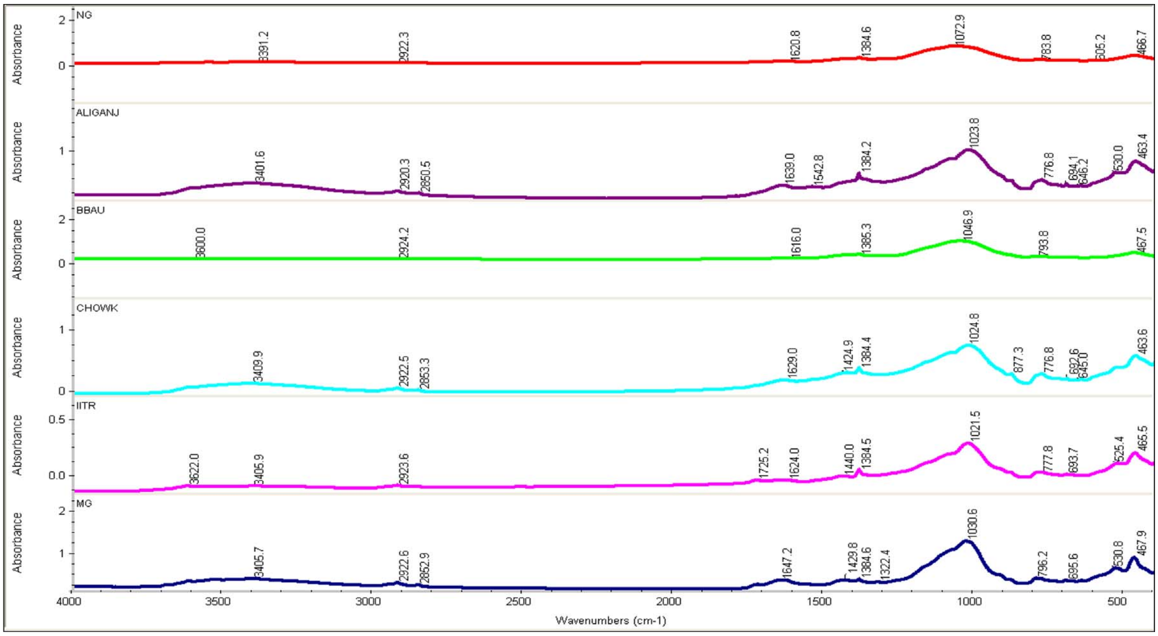

Fig. 4. FTIR spectra of particulate matter collected from various locations of Lucknow (NG = Nishatganj, MG = Mohanlalganj).

indicates the presence of silicate ions in particulate matter, whereas, absorption between 776 and 796 cm^{-1} is due to presence of silica (Manoharan et al., 2012; Nayak and Singh, 2007; Ko and Chu, 2005).

4.2. Composition of organic mass

Various functional groups present in particulates are analyzed using FTIR and the results presented in Table 3. Presence of aliphatic hydrocarbons, alcohols and carbonyl compound was seen in all the particle size fractions. The wave number around 3000–2850 characterize the aliphatic hydrocarbons due to asymmetric and symmetric C—H stretching vibration of aliphatic CH_2 group (Maria et al., 2002; Shaka and Saliba 2004), whereas, higher intensity of the band at 1384 cm^{-1} may be attributed to symmetrical C—H bending vibrations from aliphatic CH_3 (Santos and Duarte, 1998). These aliphatic carbon groups are mainly formed in the fine particle fraction of respirable dust (Anil et al., 2014). Peaks in the range of 3870-3600 and 1750–1650 cm^{-1} confirm the presence of aliphatic alcohol and carbonyl functional group. It is considered that the compounds containing the —C═O and —OH groups are the important components of secondary organic aerosol (Saxena and Hildemann, 1996). The prominent band near 1630 cm^{-1} confirms the presence of organonitrate in aerosol which may be conjugated by secondary particles emitted by fossil fuels, natural gas and residential heating (Anil et al., 2014; Shaka and Saliba 2004).

5. Conclusion

The characterizations of individual airborne particles using SEM-EDS have provided valuable information regarding the source of contaminants depending on the shape and size of the particles. Dominance of specific types of amorphous, spherical and carbonaceous particles was observed viz. organic particles with inorganic inclusion, soot, tar balls, and aluminosilicates. Various shape descriptor viz. aspect ratio, circulatory, ESD and surface area have provided the physiochemical characteristics of the particles. FTIR analysis confirmed the presence of miscellaneous functional groups viz. SO_4^{-2}, HSO^{-4}, H_2O, SiO_4^{-4}, SiO_2, NO^{-3}, SiO_4, NH_4^+, C—H, R—OH, R—O—N—O and C═O in a coarser fraction of particulate matter.

Acknowledgement

Authors are thankful to University Grant Commission (UGC), New Delhi, for providing financial assistance to Mr. Sushil Kumar Bharti in the form of Senior Research Fellowship (F.15-6 (DEC., 2011-2012). The authors also thankful to Head, Department of Environmental Science, Babasaheb Bhimrao Ambedkar University, Lucknow (BBAU), Director, University Science Instrumentation Centre (USIC), BBAU Lucknow and Director, Indian Institute of Toxicology Research (IITR), Lucknow for providing infrastructural support. The authors are grateful to Dr. Vertika Shukla for their valuable suggestion for improving the quality of manuscript.

References

Adachi, K., Buseck, P.R., 2008. Internally mixed soot, sulfates, and organic matter in aerosol particles from Mexico City. Atmos. Chem. Phys. 8, 6469–6481.

Allen, D.T., Pallen, E.J., Haimov, M.I., Hering, S.V., Young, J.R., 1994. Fourier transform infrared spectroscopy of aerosol collected in a low pressure impactor (LPI/FTIR): method development and field calibration. Aerosol Sci. Technol. 21, 325–342.

Anil, I., Golcuk, K., Karaca, F., 2014. ATR-FTIR spectroscopic study of functional groups in aerosols: the contribution of a saharan dust transport to urban atmosphere in istanbul, Turkey. Water Air Soil Pollut. 225, 1898–1909.

Begum, B.A., Hopke, P.K., Markwitz, A., 2013. Air pollution by fine particulate matter in Bangladesh. Atmos. Pollut. Res. 4, 75–86.

Berube, K.A., Jones, T.P., Williamson, B.J., Winters, C., Morgan, A.J., Richards, R.J., 1999. Physicochemical characterisation of diesel exhaust particles: Factors for assessing biological activity. Atmos. Environ. 33, 1599–1614.

Berube, K., Balharry, D., Sexton, K., Koshy, L., Jones, T., 2007. Combustion-derived nanoparticles: mechanisms of pulmonary toxicity. Clin. Exp. Pharmacol. Physiol. 34, 1044–1050.

Blanco, A.J., McIntyre, R.G., 1972. IR spectroscopic view of atmospheric particulates over El Paso. Texas Atmos. Environ. 6, 557–562.

Blando, J.D., Porcja, R.J., Li, T.H., Bowman, D., Lioy, P.J., Turpin, B.J., 1998a. Secondary formation and the Smoky Mountain organic aerosol: an examination of aerosol polarity and functional group composition during SEAVS. Environ. Sci. Technol. 32, 604–613.

Blando, J.D., Porcja, R.J., Li, T.H., Bowman, D., Lioy, P.J., Turpin, B.J., 1998b. Secondary formation and the Smoky Mountain organic aerosol: an examination of aerosol polarity and functional group composition during SEAVS. Environ. Sci. Technol. 32, 604–613.

Bond, T.C., Zarzycki, C., Flanner, M.G., Koch, D.M., 2011. Quantifying immediate radiative forcing by black carbon and organic matter with the specific forcing pulse. Atmos. Chem. Phys. 11, 1505–1525.

Brown, S., Dangler, M.C., Burke, S.R., Hering, S.V., Allen, D.T., 2007. Direct Fourier transforms Infrared Analysis of size-segregated Aerosol: results from the carbonaceous species methods Intercomparison study. Aerosol Sci. Technol. 12, 172–181.

Buseck, P., Adachi, K., Gelencser, A., Tompa, E., Posfai, M., 2012. Are black carbons and

soot the same? Atmos. Chem. Phys. Dis. 12, 24821–24846.
China, S., Mazzoleni, C., Gorkowski, K., Aiken, A.C., Dubey, M.K., 2013. Morphology and mixing state of individual freshly emitted wildfire carbonaceous particles. Nat. Commun. 4, 2122.
China, S., Salvadori, N., Mazzoleni, C., 2014. Effect of traffic and driving characteristics on morphology of atmospheric soot particles at freeway on-ramps. Environ. Sci. Technol. 48, 3128–3135.
Collins, T.J., 2007. Image J for microscopy. Biotechniques 43 (Suppl. 1), 25–30.
Cong, Z., Kang, S., Dong, S., Zhang, Y., 2009. Individual particle analysis of atmospheric aerosols at Nam Co, Tibetan Plateau. Aerosol Air Quality Res. 9, 323–331.
Cong, Z., Kang, S., Dong, S., Liu, X., Qin, D., 2010. Elemental and individual particle analysis of atmospheric aerosols from high Himalayas. Environ. Monit. Assess. 160, 323–335.
Cuadros, J., Diaz-Hernandez, J.L., Sanchez-Navas, A., Garcia- Casco, A., 2015. Role of clay minerals in the formation of atmospheric aggregates of Saharan dust. Atmos. Environ. 120, 160–172.
Deshmukh, D.K., Tsai, Y.I., Deb, M.K., Zarmpas, P., 2012a. Characteristics and sources of water soluble ionic species associated with PM_{10} particles in the ambient air of central India. Bull. Environ. Contam. Toxicol. 89, 1091–1097.
Díaz-Hernández, J.L., Párraga, J., 2008. The nature and tropospheric formation of iberulites: pinkish mineral microspherulites. Geochim. Cosmochim. Acta 72, 3883–3906.
Engelbrecht, J.P., McDonald, E.V., Gillies, J.A., Jayanty, R.K.M., Casuccio, G., Gertler, A.W., 2009a. Characterizing mineral dusts and other aerosols from the Middle East −Part 1: Ambient sampling, Inhal. Toxicol 21, 297–326.
Expert Panel on Air Quality Standards, 2001. Airborne Particles: What Is the Appropriate Measurement on Which to Base a Standard? A Discussion Document. Department for Environment. Food & Rural Affairs, London. http://www.defra.gov.uk/environment/airquality/aqs/air_measure/index.htm.
Gargava, P., Rajagopalan, V., 2016. Source apportionment studies in six Indian cities drawing broad inferences for urban PM_{10} reductions Air Quality. Atmos. Health 9 (5), 471–481.
Gilardoni, S.S., Liu, S., Takahama, L.M., Russell, J.D., Allan, R., Steinbrecher, J.L., Jimenez, P.F., Carlo De Dunlea, E.J., Baumgardner, D., 2009. Characterization of organic ambient aerosol during MIRAGE 2006 on three platforms. Atmos. Chem Phys. 9 (15), 5417–5432.
Hand, J.L., Day, D.E., McMeeking, G.M., Levin, E.J.T., Carrico, C.M., Kreidenweis, S.M., Malm, W.C., Laskin, A., Desyaterik, Y., 2010. Measured and modeled humidification factors of fresh smoke particles from biomass burning: role of inorganic constituents. Atmos. Chem. Phys. 10, 6179–6194.
Khan, M.F., Shirasuna, Y., Hirano, K., Masunaga, S., 2010. Characterization of $PM_{2.5}$, $PM_{2.5–10}$ and PM_{10} in ambient air, yokohama, Japan. Atmos. Res. 96 (1), 159–172.
Khare, P., Baruah, B.P., Rao, P.G., 2011. Water-soluble organic compounds (WSOCs) in PM (2.5) and PM (10) at a subtropical site of India. Tellus B 63, 990–1000.
Kisku, G.C., Salve, P.R., Kidwai, M.M., Khan, A.H., Barman, S.C., Singh, R., 2003. A random survey of ambient air quality in Lucknow city and its possible impact on environmental health. J. Air Pollut. Control Assoc. 3 (1), 45–58.
Ko, T.H., Chu, H., 2005. Spectroscopic study on sorption of hydrogen sulfide by mean of red soil. Spectro Chimica Acta Part-A 61, 2253–2259.
Kulkarni, P., Baron, P.A., Willeke, K., 2011. Aerosol Measurement: Principles, Techniques, and Applications, 3rd edn. Wiley, Hoboken.
Kumar, S., Verma, M.K., Srivastava, A.K., 2013. Ultrafine particles in urban ambient air and their health perspectives. Rev. Environ. Health 28, 117–128.
Lee, A.K.Y., Willis, M.D., Healy, R.M., Onasch, T.B., Abbatt, J.P.D., 2015. Mixing state of carbonaceous aerosol in an urban environment: single particle characterization using the soot particle aerosol mass spectrometer (SP-AMS). Atmos. Chem. Phys. 15, 1823–1841.
Levin, M., Witschger, O., Bau, S., Jankowska, E., Koponen, I.K., Koivisto, A.J., Clausen, P.A., Jensen, A., Mølhave, K., Asbach, C., 2016. Can we trust real time measurements of lung deposited surface area concentrations in dust from powder nanomaterials? Aerosol Air Qual. Res. 16, 1105–1117.
Li, J., Posfai, M., Hobbs, P.V., Buseck, P.R., 2003. Individual aerosol particles from biomass burning in southern Africa: 2, Compositions and aging of inorganic particles. J. Geophys. Res.-Atmos. 108 (D13). http://dx.doi.org/10.1029/2002JD002310.
Manoharan, C.P., Sutharsan, S., Dhanapandian Venkatachalapathy, R., 2012. Spectroscopic and thermal analysis of red clay for industrial applications from Tamilnadu, India. J. Mol. Struct. 1027, 99–103.
Maria, S.F., Russell, L.M., Turpin, B.J., Porcja, R.J., 2002. FTIR measurements of functional groups and organic mass in aerosol samples over the Caribbean. Atmos. Environ. 36, 5185–5196.
Mishra, S.K., Agnihotri, R., Yadav, P.K., Singh, S., Prasad, M.V.S.N., Praveen, P.S., Tawale, J.S., Rashmi Mishra, N.D., Arya, B.C., Sharma, C., 2015. Morphology of atmospheric particles over semi-Arid region (Jaipur, rajasthan) of India: implications for optical properties. Aerosol Air Qual. Res. 15, 974–984.
Moffet, R.C., Brien, R.E., Alpert, P.A., Kelly, S.T., Pham, D.Q., Gilles, M.K., Knopf, D.A., Laskin, A., 2016. Morphology and mixing of black carbon particles collected in central California during the CARES field study. Atmos. Chem. Phys. 16, 14515–14525.
Murari, V., Kumar, M., Singh, N., Singh, R.S., Banerjee, T., 2016. Particulate morphology and elemental characteristics: variability at middle Indo-Gangetic Plain. J. Atmos. Chem. 73, 165–179.
NAAQS, 2009. CPCB: NAAQS, The Gazette of India: Central Pollution Control Board. Ministry of Environment & Forests New Delhi, India.
Nayak, P.S., Singh, B.K., 2007. Instrumental characterization of clay by XRF, XRD and FTIR. Bull. Mater. Sci. 30, 235–238.
Pipal, A.S., Kulshrestha, A., Taneja, A., 2011. Characterization and morphological analysis of airborne $PM_{2.5}$ and PM_{10} in Agra located in north central India. Atoms. Environ. 45, 3621–3630.
Posfai, M., Molnar, A., 2000. Aerosol particles in the troposphere: A mineralogical introduction. EMU Notes Miner. 2, 197–252.
Pósfai, M., Buseck, P.R., 2010. Nature and climate effects of individual tropospheric aerosol particles. Annu. Rev. Earth Planet Sci. 38, 17–43.
Posfai, M., Anderson, J.R., Buseck, P.R., Sievering, H., 1999. Soot and sulfate aerosol particles in the remote marine troposphere. J. Geophys. Res. 104 (D17), 21685–21693. http://dx.doi.org/10.1029/1999JD900208.
Pósfai, M., Simonics, R., Li, J., Hobbs, P.V., Buseck, P.R., 2003. Individual aerosol particles from biomass burning in southern Africa 1. Compositions and size distributions of carbonaceous particles. J. Geophys. Res. 108 (D13), 8483. http://dx.doi.org/10.1029/2002JD002291.
Ram, S.S., Majumdar, S., Chaudhuri, P., Chanda, S., Santra, S.C., Maiti, P.K., Sudarshan, M., Chakraborty, A., 2012. SEM EDS: an important tool for air pollutant biomonitoring. Micron 43, 490–493.
Santos, E.B.H., Duarte, A.C., 1998. The influence of pulp and paper mill effluent on the composition of the humic fraction of aquatic organic matter. Water Res. 32 (3), 597–608.
Satsangi, P.G., Yadav, S., 2014. Characterization of PM2. 5 by X-ray diffraction and scanning electron microscopy–energy dispersive spectrometer: its relation with different pollution sources. Int. J. Environ. Sci. Technol. 11, 217–232.
Saxena, P., Hildemann, L., 1996. Water-soluble organics in atmospheric particles: a critical review of the literature and application of thermodynamics to identify candidate compounds. J. Atmos. Chem. 24, 57–109.
Scheuvens, D., Kandler, K., Küpper, M., Lieke, K., Zorn, S.R., Ebert, M., Schütz, L., Weinbruch, S., 2011. Individual-particle analysis of airborne dust samples collected over Morocco in 2006 during SAMUM 1. Tellus B 63, 512–530.
Seinfeld, J.H., Pandis, S.N., 1998. Atmospheric Chemistry and Physics. John Wiley and Sons Inc, New York.
Shaka, H., Saliba, N.A., 2004. Concentration measurements and chemical composition of PM_{10} and $PM_{2.5}$ at a coastal site in Beirut, Lebanon. Atmos. Environ. 38, 523–531.
Sharma, S.G., Srinivas, M.S.N., 2008. Study of chemical composition and morphology of airborne particles in Chandigarh, India using EDXRF and SEM techniques. Environ. Monit. Assess. 150 (1–4), 417–425. http://dx.doi.org/10.1007/s10661-008-0240-7.
Sharma, K., Singh, R., Barman, S.C., Mishra, D., Kumar, R., Negi, M.P.S., 2006. Comparison of trace metals concentration in PM10 of different location of Lucknow city. Bull. Environ. Contam. Toxicol. 77, 419–426.
Sharma, S.K., Mandal, T.K., Srivastava, M.K., Chatterjee, A., Jain, S., Saxena, M., Singh, B.P., Saraswati, A., Sharma, A., Adak, A., Ghosh, S.K., 2016. Spatio-temporal variation in chemical characteristics of PM_{10} over Indo Gangetic Plain of India. Environ. Sci. Pollut. Res. 23 (18), 18809–18822.
Sielicki, P., Janik, H., Guzman, A., Namiesnik, J., 2011. The progress in electron microscopy studies of particulate matters to be used as a standard monitoring method for air dust pollution. Crit. Rev. Anal. Chem. 41, 314–334.
Singh, N., Mhawish, A., Debuoudt, K., Singh, R.S., Banerjee, T., 2017. Organic aerosols over Indo- Gangetic Plain: Sources, distributions and climatic implications. Atmos. Environ. 157, 59–74.
Slezakova, K., Pires, J.C.M., Pereira, M.C., Martins, F.G., Alvim-Ferraz, M.C., 2008. Influence of traffic emissions on the composition of atmospheric particles of different sizes-Part 2: SEM–EDS characterization. J. Atmos. Chem. 60 (3), 221–236.
Song, X., Yang, S., Shao, L., et al., 2016. PM_{10} mass concentration, chemical composition, and sources in the typical coal-dominated industrial city of Pingdingshan, China. Sci. Total Environ. 571, 1155–1163. http://dx.doi.org/10.1016/j.scitotenv.2016.07.115.
Srivastava, A., Jain, V.K., Srivastava, A., 2009. SEM-EDX analysis of various sizes aerosols in Delhi India. Environ. Monit. Assess. 150, 405–416.
Stevanovic, S., Miljevic, B., Surawski, N., Fairfull-Smith, K., Bottle, S., Brown, R., Ristovski, Z., 2013. Influence of oxygenated organic aerosols (OOAs) on the oxidative potential of diesel and biodiesel particulate matter. Environ. Sci Technol. 47 (14), 7655–7662.
Strak, M., Janssen, N.A., Godri, K.J., Gosens, I., Mudway, I.S., Cassee, F.R., 2012. Respiratory health effects of airborne particulate matter: the role of particle size, composition, and oxidative potential—the RAPTES project. Environ. Health Perspect. 120, 1183–1189.
Tecer, L.H., Tomac, N., Karaca, F., Kaplan, A., Tuncer, T., Aydin, H., 2009. The evaluation of the effect of air pollution on the health status of children in Zonguldak city, Turkey. Int. J. Environ. Pollut. 39 (3–4), 352–364.
Tivanski, A.V., Hopkins, R.J., Tyliszczak, T., Gilles, M.K., 2007. Oxygenated interface on biomass burn tar balls determined by single particle scanning transmission X-ray microscopy. J. Phys. Chem. A 111, 5448–5458.
Tiwari, S., Srivastava, A.K., Bisht, D.S., Safai, P.D., Parmita, P., 2012. Assessment of carbonaceous aerosol over delhi in the indo-Gangetic basin: characterization, sources and temporal variability. Nat. Hazards 65, 1745–1764.
Tiwari, S., Pandithurai, G., Attri, S.D., Srivastava, A.K., Soni, V.K., Bisht, D.S., Kumar, A.V., Srivastava, M.K., 2015. Aerosol optical properties and their relationship with meteorological parameters during winter time in Delhi, India. Atmos. Res. 153, 465–479.
Tiwary, A., Reff, A., Colls, J.J., 2008. Collection of ambient particulate matter by porous vegetation barriers: sampling and characterization methods. J. Aerosol Sci. 39, 40–47.
Toledo, V.E., Almeida, P.B., Quiterio, S.L., et al., 2008. Evaluation of levels, sources and distribution of toxic elements in PM10 in a suburban industrial region, Rio de Janeiro, Brazil. Environ. Monit. Assess. 139, 49–59.
Tumolva, L., Park, J.Y., Kim, J., Miller, A.L., Chow, J.C., Watson, J.G., Park, K., 2010. Morphological and Elemental classification of freshly emitted soot particles and atmospheric ultrafine particles using the TEM/EDS. Aerosol Sci. Technol. 44, 202–215.
USEPA, 2017. National Ambient Air Quality Standards (NAAQS). US Environmental

Protection Agency, 2012. available at: http://www.epa.gov/air/criteria.html (last access: 24 August 2017).
Verma, M.K., Chauhan, L.K.S., Sultana, S., Kumar, S., 2014. The traffic linked urban ambient air superfine and ultrafine PM_1 mass concentration, contents of pro–oxidant chemicals, and their seasonal drifts in Lucknow, India. Atmos. Pollut. Res. 5, 677–685.
WHO, 2005. WHO Air Quality Guidelines Global Update. Particulate Matter, Ozone, Nitrogen Dioxide and Sulphur Dioxide. World Health Organization, Regional office of Europe, Copenhagen. available at: http:// www.euro.who.int/Document/E90038.pdf, Last access at 12 June 2017.
WHO, 2014. Burden of Disease from Ambient Air Pollution for 2012. World Health Organization Geneva, Switzerland. http://www.who. Int/phe/health_topics/outdoorair/databases/AAP_BoD_results_ March2014. pdf.
Wu, Z., Hu, M., Lin, P., Liu, S., Wehner, B., Wiedensohler, A., 2008. Particle number size distribution in the urban atmosphere of Beijing, China. Atoms. Environ. 42, 7967–7980.
Wu, S.F., Deng, X., Wang, H., Wei, M., Shima, J., Huang, H., Lu, Y., Hao, C., Zheng, Y., Qin, X., Lu, X., Guo, 2013. Association of lung function in a panel of young healthy adults with various chemical components of ambient fine particulate air pollution in beijing, China. Atmos. Environ. 77, 873–884.
Zhang, Y., Yu, Q., Ma, W., Chen, L., 2010. Atmospheric deposition of inorganic nitrogen to the eastern China seas and its implications to marine biogeochemistry. J. Geophys. Res. 115, D00K10.
Zhou, H., He, J., Zhao, B., et al., 2016. The distribution of PM_{10} and $PM_{2.5}$ carbonaceous aerosol in Baotou, China. Atmos Res. 178–179, 102–113. http://dx.doi.org/10.1016/j.atmosres.2016.03.019.